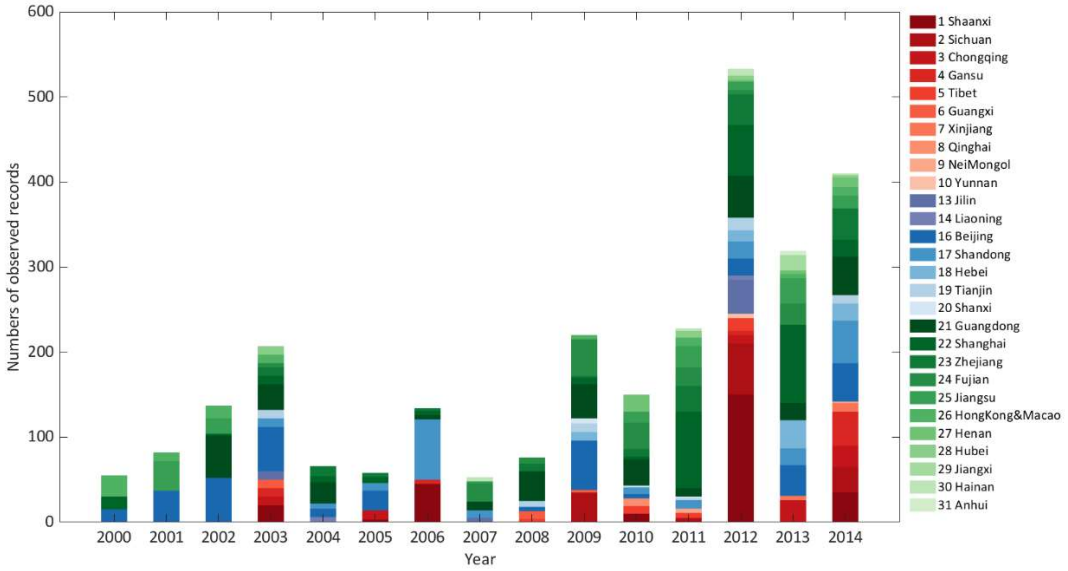

Figure S1. Provincial observed records over China during 2000–2014. The color and labeling of provinces are consistent with Figure 1.

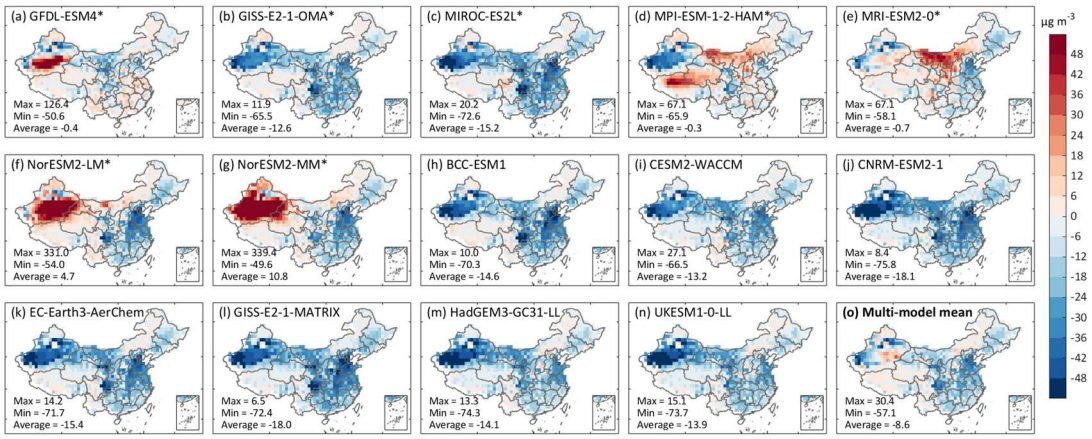

Figure S2. Spatial distribution of bias in the multi-year average of simulate-based $PM_{2.5}$ concentrations during 2000–2014 for each model.

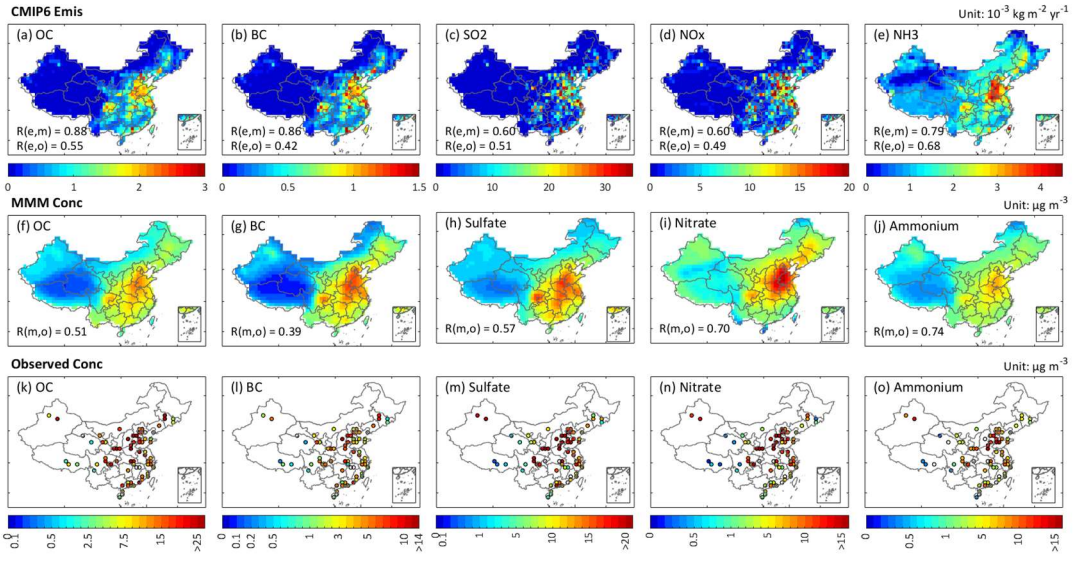

Figure S3. Multi-year average of CMIP6 emissions (a-e), multi-model mean concentrations (f-j), and observed concentrations (k-o) of air pollutants over 2000–2014. R (e, m), R (e, o), and R (m, o) denote the spatial correlation coefficients between CMIP6 emissions and multi-model mean concentrations, between CMIP6 emissions and observed concentrations, and between multi-model mean concentrations and observed concentrations.

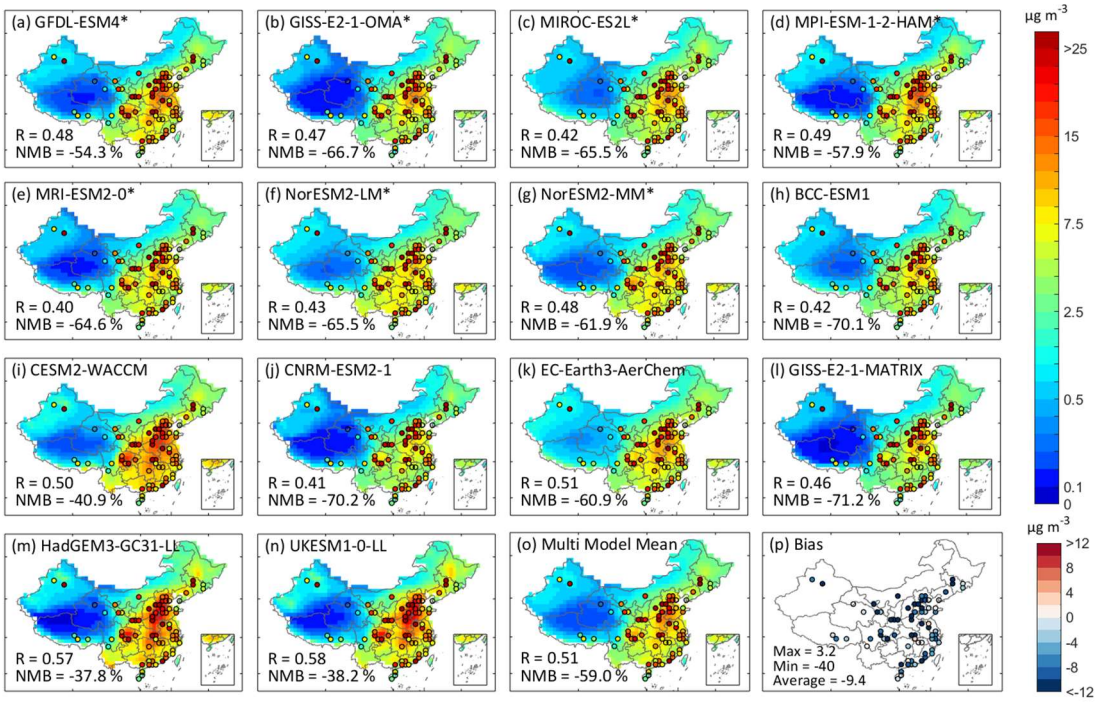

Figure S4. Multi-year mean annual average near-surface OC concentrations over China during 2000–2014. (a-n) OC in individual models overlaid with ground-based observations. (o) Multi-model mean overlaid with ground-based observations. (p) Bias in multi-model mean.

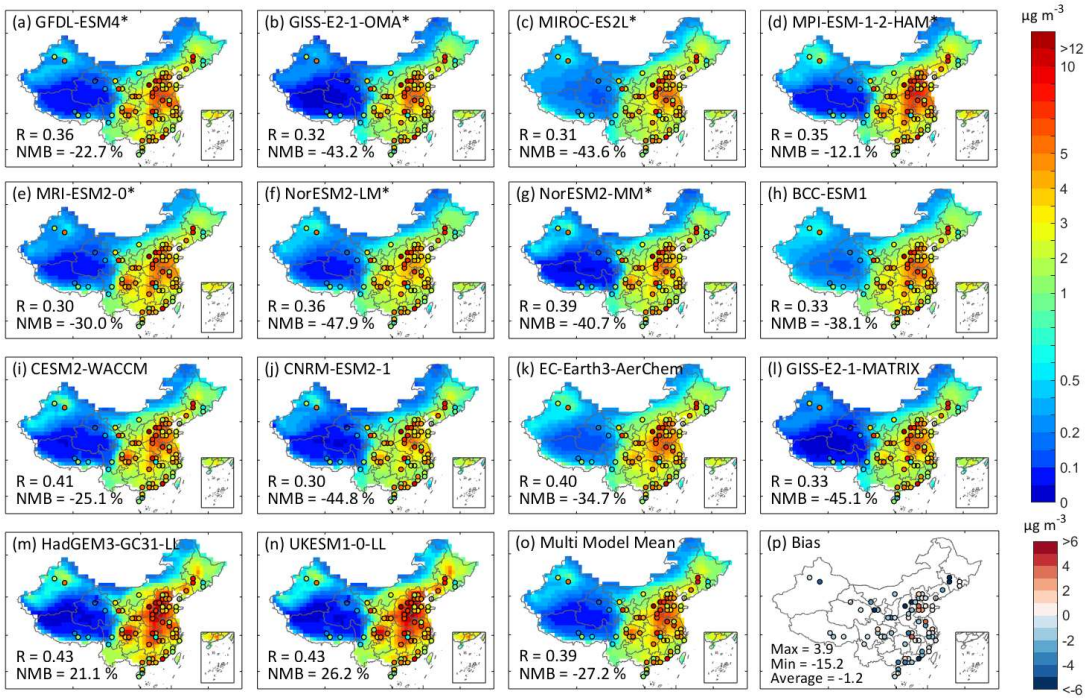

Figure S5. Multi-year mean annual average near-surface BC concentrations over China during 2000–2014. (a-n) BC in individual models overlaid with ground-based observations. (o) Multi-model mean overlaid with ground-based observations. (p) Bias in multi-model mean.

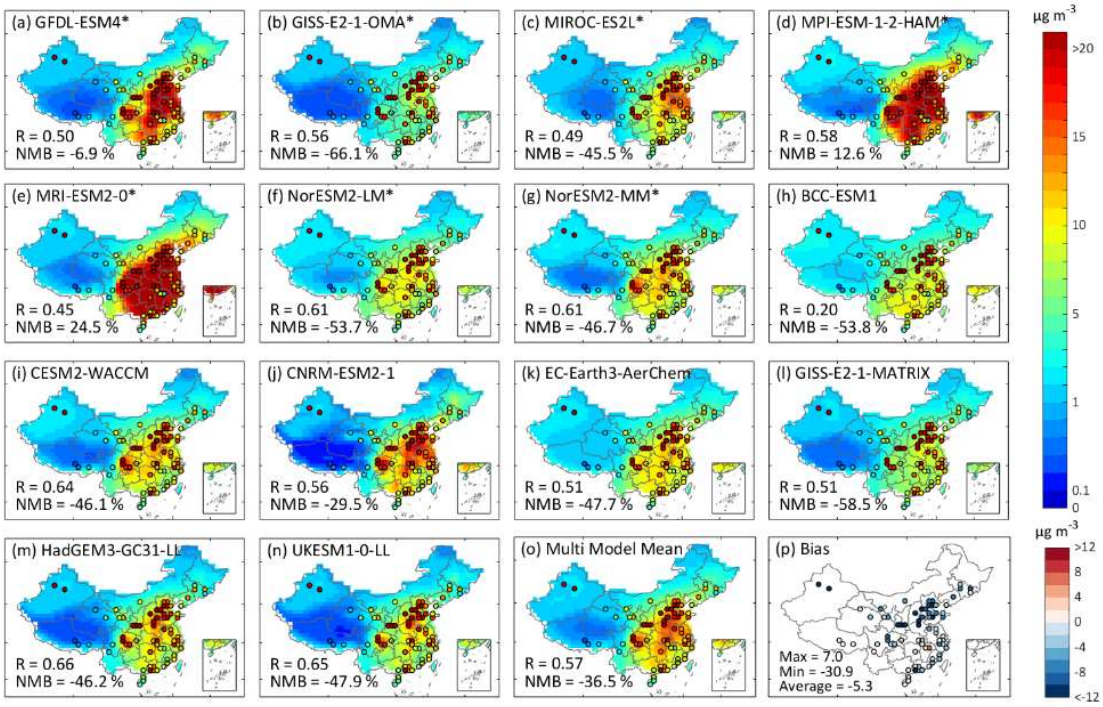

Figure S6. Multi-year mean annual average near-surface sulfate concentrations over China during 2000–2014. (a-n) Sulfate in individual models overlaid with ground-based observations. (o) Multi-model mean overlaid with ground-based observations. (p) Bias in multi-model mean.

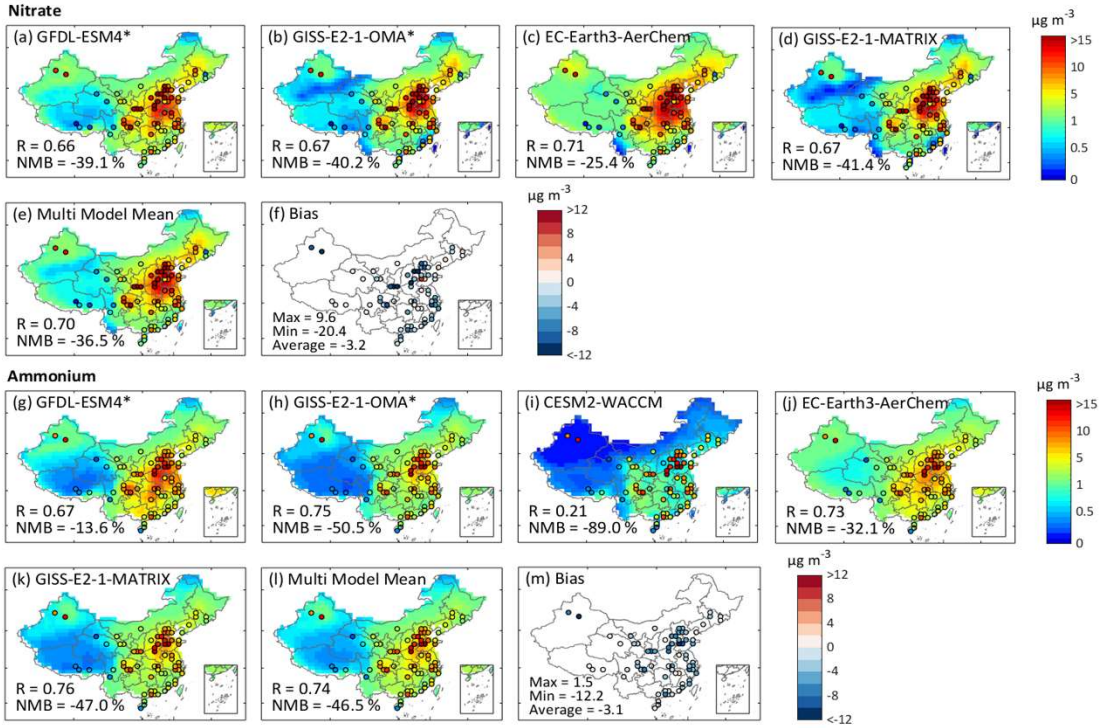

Figure S7. Multi-year mean annual average near-surface nitrate and ammonium concentrations over China during 2000–2014. (a-d) Nitrate and (g-k) ammonium in individual models overlaid with ground-based observations. (e, l) Multi-model mean of overlaid with ground-based observations. (f, m) Bias in multi-model mean.

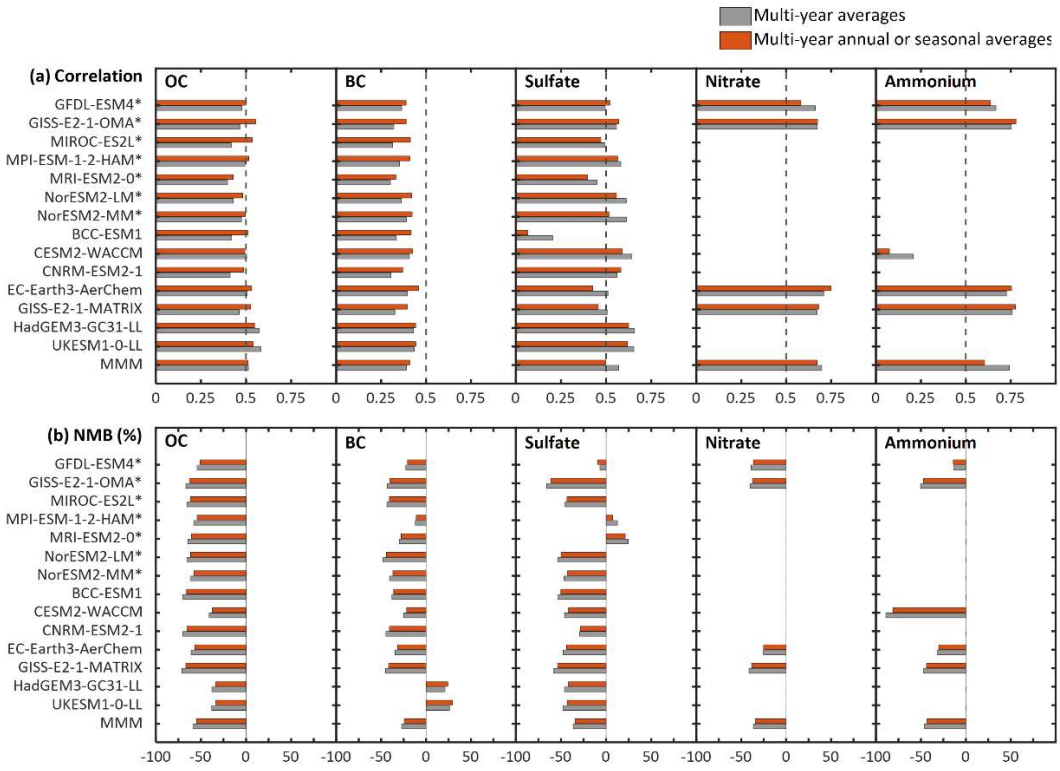

Figure S8. Spatial correlation and bias of multi-year averages (gray bar) and multi-year annual or seasonal averages

(red bar) of $PM_{2.5}$ components during 2000–2014 for individual models.

Table S1. CMIP6 models and $PM_{2.5}$ outputs.

Model	Resolution (Lat × Lon)	Number of members	OA, BC, SO_4^{2-}, SSLT, DST	NO_3^-, NH_4^+	$PM_{2.5}$	Model references and data citation
BCC-ESM1	2.813° × 2.813°	3	Y			(Wu et al., 2019; Wu et al., 2020; Zhang et al., 2018)
CESM2-WACCM	0.9° × 1.25°	3	Y	Y (No NO_3^-)		(Danabasoglu, 2019; Gettelman et al., 2019; Tilmes et al., 2019; Emmons et al., 2020)
CNRM-ESM2-1	1.4°× 1.4°	3	Y			(Séférian, 2018; Séférian et al., 2019; Michou et al., 2020)
EC-Earth3-AerChem	2° × 3°	3	Y	Y		(Van Noije et al., 2021; Döscher et al., 2022; EC-Earth Ec-Earth-Consortium, 2020)
GFDL-ESM4	1° × 1.25°	1	Y	Y	Y	(Horowitz et al., 2020; Dunne et al., 2020; Krasting et al., 2018)
GISS-E2-1-OMA	2° × 2.5°	15	Y	Y	Y	(Bauer et al., 2020; Miller et al., 2021; Nasa Goddard Institute for Space Studies, 2018)
GISS-E2-1-MATRIX	2° × 2.5°	12	Y	Y		(Bauer et al., 2020; Miller et al., 2021; Nasa Goddard Institute for Space Studies, 2018)
HadGEM3-GC31-LL	1.25° × 1.875°	4	Y			(Ridley et al., 2018; Kuhlbrodt et al., 2018)
MIROC-ES2L	2.813° × 2.813°	10	Y		Y	(Hajima et al., 2020; Hajima et al., 2019)
MPI-ESM-1-2-HAM	1.875° × 1.875°	3	Y		Y	(Tegen et al., 2019; Neubauer et al., 2019)
MRI-ESM2-0	1.875° × 1.875°	5	Y		Y	(Yukimoto et al., 2019a; Yukimoto et al., 2019b; Oshima et al., 2020)

NorESM2-LM	1.9° × 2.5°	3	Y	Y	(Karset et al., 2018; Seland et al., 2019; Seland et al., 2020; Kirkevåg et al., 2018)
NorESM2-MM	0.9° × 1.25°	3	Y	Y	(Karset et al., 2018; Bentsen et al., 2019; Seland et al., 2020; Kirkevåg et al., 2018)
UKESM1-0-LL	1.25° × 1.875°	4	Y		(Tang et al., 2019; Sellar et al., 2019)

Table S2. The specific values of a_1 and a_2 from Eq. 1. The average, trend, and spatial correlation coefficients of $PM_{2.5}$ concentrations over the eastern region and western region during 2000−2014.

	Model	a_1	a_2	Eastern region			Western region		
				Average (μg m^{-3})	Trend (μg m^{-3} yr^{-1})[a]	Spatial Corr.[b]	Average (μg m^{-3})	Trend (μg m^{-3} yr^{-1})	Spatial Corr.
Satellite-based				39.0	0.72	1	22.7	0.06*	1
Total $PM_{2.5}$ from Direct ESM output	GFDL-ESM4			37.7	1.14	0.92	22.1	0.28	0.66
	GISS-E2-1-OMA			24.4	0.69	0.91	10.9	0.13	0.79
	MIROC-ES2L			20.3	0.49	0.90	8.9	0.13	0.59
	MPI-ESM-1-2-HAM			36.6	0.93	0.91	22.5	0.20*	0.36
	MRI-ESM2-0			30.4	0.57	0.83	24.5	0.24	0.71
	NorESM2-LM			22.1	0.32	0.87	35.5	0.03*	0.49
	NorESM2-MM			23.6	0.40	0.90	43.1	–0.10*	0.53
Total $PM_{2.5}$ from Eq. 1	BCC-ESM1			19.5	0.40	0.87	10.2	0.15	0.62
	CESM2-WACCM	0.25	0.1	24.0	0.73	0.92	10.1	0.22	0.67
	CNRM-ESM2-1	0.02	0.25	18.9	0.42	0.90	5.5	0.11	0.51
	EC-Earth3-AerChem	0.25	0.1	21.4	0.56	0.91	8.3	0.18	0.53

	GISS-E2-1-MATRIX	0.25	0.1	17.0	0.43	0.92	6.4	0.10	0.67
	HadGEM3-GC31-LL	0.27	0.35	26.5	0.80	0.89	7.9	0.18	0.50
	UKESM1-0-LL	0.27	0.35	26.5	0.71	0.89	8.1	0.18	0.52

[a] Trends are estimated using the Theil-Sen Median method (Theil, 1950; Sen, 1968). Significant changes are identified using the non-parametric Mann-Kendall test (Kendall, 1938). * represents non-significant monotonous change at $p = 0.05$. [b] Spatial correlation coefficients between simulations and satellite-based data over the eastern and western regions are calculated. The spatial correlation coefficients of 14 models are at the 0.05 significance level.

Table S3. Multi-year averages of $PM_{2.5}$ concentrations including five aerosol species (Eq. 1) and all fine aerosol species from 4 models providing nitrate and ammonium simulations.

Model	$PM_{2.5}$ according to Eq. 1 (μg m^{-3})	$PM_{2.5}$ including all fine aerosol species (μg m^{-3})[a]	Nitrate proportion[b]	Ammonium proportion
EC-Earth3-AerChem	12.1	18.7	20.6%	14.3%
GFDL-ESM4	13.0	18.5	15.1%	14.6%
GISS-E2-1-OMA	10.0	14.1	17.6%	11.4%
GISS-E2-1-MATRIX	9.5	13.8	17.5%	13.2%

[a] represents that $PM_{2.5} = OA + BC + SO_4^{2-} + 0.25SSLT + 0.1DST + NO_3^- + NH_4^+$. [b] represents that the proportion of nitrate to $PM_{2.5}$ including all fine aerosol species.

Reference

Bauer, S. E., Tsigaridis, K., Faluvegi, G., Kelley, M., Lo, K. K., Miller, R. L., Nazarenko, L., Schmidt, G. A., and Wu, J.: Historical (1850–2014) Aerosol Evolution and Role on Climate Forcing Using the GISS ModelE2.1 Contribution to CMIP6, J. Adv. Model. Earth Syst., 12, e2019MS001978, https://doi.org/10.1029/2019MS001978, 2020.

Bentsen, M., Oliviè, D. J. L., Seland, Ø., Toniazzo, T., Gjermundsen, A., Graff, L. S., Debernard, J. B., Gupta, A. K., He, Y., Kirkevåg, A., Schwinger, J., Tjiputra, J., Aas, K. S., Bethke, I., Fan, Y., Griesfeller, J., Grini, A., Guo, C., Ilicak, M., Karset, I. H. H., Landgren, O. A., Liakka, J., Moseid, K. O., Nummelin, A., Spensberger, C., Tang, H., Zhang, Z., Heinze, C., Iversen, T., and Schulz, M.: NCC NorESM2-MM model output prepared for CMIP6 CMIP (v20201001), Earth System Grid Federation [dataset], https://doi.org/10.22033/ESGF/CMIP6.506, 2019.

Danabasoglu, G.: NCAR CESM2-WACCM model output prepared for CMIP6 CMIP (v20190415), Earth System Grid Federation [dataset], https://doi.org/10.22033/ESGF/CMIP6.10024, 2019.

Döscher, R., Acosta, M., Alessandri, A., Anthoni, P., Arsouze, T., Bergman, T., Bernardello, R., Boussetta, S., Caron, L. P., Carver, G., Castrillo, M., Catalano, F., Cvijanovic, I., Davini, P., Dekker, E., Doblas-Reyes, F. J., Docquier, D., Echevarria, P., Fladrich, U., Fuentes-Franco, R., Gröger, M., v. Hardenberg, J., Hieronymus, J., Karami, M. P., Keskinen, J. P., Koenigk, T., Makkonen, R., Massonnet, F., Ménégoz, M., Miller, P. A., Moreno-Chamarro, E., Nieradzik, L., van Noije, T., Nolan, P., O'Donnell, D., Ollinaho, P., van den Oord, G., Ortega, P., Prims, O. T., Ramos, A., Reerink, T., Rousset, C., Ruprich-Robert, Y., Le Sager, P., Schmith, T., Schrödner, R., Serva, F., Sicardi, V., Sloth Madsen, M., Smith, B., Tian, T., Tourigny, E., Uotila, P., Vancoppenolle, M., Wang, S., Wårlind, D., Willén, U., Wyser, K., Yang, S., Yepes-Arbós, X., and Zhang, Q.: The EC-Earth3 Earth system model for the Coupled Model Intercomparison Project 6, Geosci. Model Dev., 15, 2973-3020, https://doi.org/10.5194/gmd-15-2973-2022, 2022.

Dunne, J. P., Horowitz, L. W., Adcroft, A. J., Ginoux, P., Held, I. M., John, J. G., Krasting, J. P., Malyshev, S., Naik, V., Paulot, F., Shevliakova, E., Stock, C. A., Zadeh, N., Balaji, V., Blanton, C., Dunne, K. A., Dupuis, C., Durachta, J., Dussin, R., Gauthier, P. P. G., Griffies, S. M., Guo, H., Hallberg, R. W., Harrison, M., He, J., Hurlin, W., McHugh, C., Menzel, R., Milly, P. C. D., Nikonov, S., Paynter, D. J., Ploshay, J., Radhakrishnan, A., Rand, K., Reichl, B. G., Robinson, T., Schwarzkopf, D. M., Sentman, L. T., Underwood, S., Vahlenkamp, H., Winton, M., Wittenberg, A. T., Wyman, B., Zeng, Y., and Zhao, M.: The GFDL Earth System Model Version 4.1 (GFDL-ESM 4.1): Overall Coupled Model Description and Simulation Characteristics, J. Adv. Model. Earth Syst., 12, e2019MS002015, https://doi.org/10.1029/2019MS002015, 2020.

EC-Earth-Consortium: EC-Earth3-AerChem model output prepared for CMIP6 CMIP (v20201214), Earth System Grid Federation [dataset], https://doi.org/10.22033/ESGF/CMIP6.639, 2020.

Emmons, L. K., Schwantes, R. H., Orlando, J. J., Tyndall, G., Kinnison, D., Lamarque, J.-F., Marsh, D., Mills, M. J., Tilmes, S., Bardeen, C., Buchholz, R. R., Conley, A., Gettelman, A., Garcia, R., Simpson, I., Blake, D. R., Meinardi, S., and Pétron, G.: The Chemistry Mechanism in the Community Earth System Model Version 2 (CESM2), J. Adv. Model. Earth Syst., 12, e2019MS001882, https://doi.org/10.1029/2019MS001882, 2020.

Gettelman, A., Mills, M. J., Kinnison, D. E., Garcia, R. R., Smith, A. K., Marsh, D. R., Tilmes, S., Vitt, F., Bardeen, C. G., McInerny, J., Liu, H.-L., Solomon, S. C., Polvani, L. M., Emmons, L. K., Lamarque, J.-F., Richter, J. H., Glanville, A. S., Bacmeister, J. T., Phillips, A. S., Neale, R. B., Simpson, I. R., DuVivier, A. K., Hodzic, A., and Randel, W. J.: The Whole Atmosphere Community Climate Model Version 6 (WACCM6), J. Geophys. Res.-Atmos., 124, 12380-12403, https://doi.org/10.1029/2019JD030943, 2019.

Hajima, T., Watanabe, M., Yamamoto, A., Tatebe, H., Noguchi, M. A., Abe, M., Ohgaito, R., Ito, A., Yamazaki, D., Okajima, H., Ito, A., Takata, K., Ogochi, K., Watanabe, S., and Kawamiya, M.: Development of the MIROC-ES2L Earth system model and the evaluation of biogeochemical processes and feedbacks, Geosci. Model Dev., 13, 2197-2244, https://doi.org/10.5194/gmd-13-2197-2020, 2020.

Hajima, T., Abe, M., Arakawa, O., Suzuki, T., Komuro, Y., Ogura, T., Ogochi, K., Watanabe, M., Yamamoto, A., Tatebe, H., Noguchi, M. A., Ohgaito, R., Ito, A., Yamazaki, D., Ito, A., Takata, K., Watanabe, S., Kawamiya, M., and Tachiiri, K.: MIROC MIROC-ES2L model output prepared for CMIP6

CMIP (v20190823), Earth System Grid Federation [dataset], https://doi.org/10.22033/ESGF/CMIP6.902, 2019.

Horowitz, L. W., Naik, V., Paulot, F., Ginoux, P. A., Dunne, J. P., Mao, J., Schnell, J., Chen, X., He, J., John, J. G., Lin, M., Lin, P., Malyshev, S., Paynter, D., Shevliakova, E., and Zhao, M.: The GFDL Global Atmospheric Chemistry-Climate Model AM4.1: Model Description and Simulation Characteristics, J. Adv. Model. Earth Syst., 12, e2019MS002032, https://doi.org/10.1029/2019MS002032, 2020.

Karset, I. H. H., Berntsen, T. K., Storelvmo, T., Alterskjær, K., Grini, A., Olivié, D., Kirkevåg, A., Seland, Ø., Iversen, T., and Schulz, M.: Strong impacts on aerosol indirect effects from historical oxidant changes, Atmos. Chem. Phys., 18, 7669-7690, https://doi.org/10.5194/acp-18-7669-2018, 2018.

Kendall, M. G.: A new measure of rank correlation, Biometrika, 30, 81-93, https://doi.org/10.1093/biomet/30.1-2.81, 1938.

Kirkevåg, A., Grini, A., Olivié, D., Seland, Ø., Alterskjær, K., Hummel, M., Karset, I. H. H., Lewinschal, A., Liu, X., Makkonen, R., Bethke, I., Griesfeller, J., Schulz, M., and Iversen, T.: A production-tagged aerosol module for Earth system models, OsloAero5.3 – extensions and updates for CAM5.3-Oslo, Geosci. Model Dev., 11, 3945-3982, https://doi.org/10.5194/gmd-11-3945-2018, 2018.

Krasting, J. P., John, J. G., Blanton, C., McHugh, C., Nikonov, S., Radhakrishnan, A., Rand, K., Zadeh, N. T., Balaji, V., Durachta, J., Dupuis, C., Menzel, R., Robinson, T., Underwood, S., Vahlenkamp, H., Dunne, K. A., Gauthier, P. P. G., Ginoux, P., Griffies, S. M., Hallberg, R., Harrison, M., Hurlin, W., Malyshev, S., Naik, V., Paulot, F., Paynter, D. J., Ploshay, J., Reichl, B. G., Schwarzkopf, D. M., Seman, C. J., Silvers, L., Wyman, B., Zeng, Y., Adcroft, A., Dunne, J. P., Dussin, R., Guo, H., He, J., Held, I. M., Horowitz, L. W., Lin, P., Milly, P. C. D., Shevliakova, E., Stock, C., Winton, M., Wittenberg, A. T., Xie, Y., and Zhao, M.: NOAA-GFDL GFDL-ESM4 model output prepared for CMIP6 CMIP (v20190726), Earth System Grid Federation [dataset], https://doi.org/10.22033/ESGF/CMIP6.1407, 2018.

Kuhlbrodt, T., Jones, C. G., Sellar, A., Storkey, D., Blockley, E., Stringer, M., Hill, R., Graham, T., Ridley, J., Blaker, A., Calvert, D., Copsey, D., Ellis, R., Hewitt, H., Hyder, P., Ineson, S., Mulcahy, J., Siahaan, A., and Walton, J.: The Low-Resolution Version of HadGEM3 GC3.1: Development and Evaluation for Global Climate, J. Adv. Model. Earth Syst., 10, 2865-2888, https://doi.org/10.1029/2018MS001370, 2018.

Michou, M., Nabat, P., Saint-Martin, D., Bock, J., Decharme, B., Mallet, M., Roehrig, R., Séférian, R., Sénési, S., and Voldoire, A.: Present-Day and Historical Aerosol and Ozone Characteristics in CNRM CMIP6 Simulations, J. Adv. Model. Earth Syst., 12, e2019MS001816, https://doi.org/10.1029/2019MS001816, 2020.

Miller, R. L., Schmidt, G. A., Nazarenko, L. S., Bauer, S. E., Kelley, M., Ruedy, R., Russell, G. L., Ackerman, A. S., Aleinov, I., Bauer, M., Bleck, R., Canuto, V., Cesana, G., Cheng, Y., Clune, T. L., Cook, B. I., Cruz, C. A., Del Genio, A. D., Elsaesser, G. S., Faluvegi, G., Kiang, N. Y., Kim, D., Lacis, A. A., Leboissetier, A., LeGrande, A. N., Lo, K. K., Marshall, J., Matthews, E. E., McDermid, S., Mezuman, K., Murray, L. T., Oinas, V., Orbe, C., Pérez García-Pando, C., Perlwitz, J. P., Puma, M. J., Rind, D., Romanou, A., Shindell, D. T., Sun, S., Tausnev, N., Tsigaridis, K., Tselioudis, G., Weng, E., Wu, J., and

Yao, M.-S.: CMIP6 Historical Simulations (1850–2014) With GISS-E2.1, J. Adv. Model. Earth Syst., 13, e2019MS002034, https://doi.org/10.1029/2019MS002034, 2021.

Nasa Goddard Institute for Space Studies: NASA-GISS GISS-E2.1G model output prepared for CMIP6 CMIP (v20190702), Earth System Grid Federation [dataset], https://doi.org/10.22033/ESGF/CMIP6.1400, 2018.

Neubauer, D., Ferrachat, S., Siegenthaler-Le Drian, C., Stoll, J., Folini, D. S., Tegen, I., Wieners, K.-H., Mauritsen, T., Stemmler, I., Barthel, S., Bey, I., Daskalakis, N., Heinold, B., Kokkola, H., Partridge, D., Rast, S., Schmidt, H., Schutgens, N., Stanelle, T., Stier, P., Watson-Parris, D., and Lohmann, U.: HAMMOZ-Consortium MPI-ESM1.2-HAM model output prepared for CMIP6 CMIP (v20190627), Earth System Grid Federation [dataset], https://doi.org/10.22033/ESGF/CMIP6.1622, 2019.

Oshima, N., Yukimoto, S., Deushi, M., Koshiro, T., Kawai, H., Tanaka, T., and Yoshida, K.: Global and Arctic effective radiative forcing of anthropogenic gases and aerosols in MRI-ESM2.0, Prog. Earth Planet. Sci., 7, https://doi.org/10.1186/s40645-020-00348-w, 2020.

Ridley, J., Menary, M., Kuhlbrodt, T., Andrews, M., and Andrews, T.: MOHC HadGEM3-GC31-LL model output prepared for CMIP6 CMIP (v20190624), Earth System Grid Federation [dataset], https://doi.org/10.22033/ESGF/CMIP6.419, 2018.

Séférian, R.: CNRM-CERFACS CNRM-ESM2-1 model output prepared for CMIP6 CMIP (v20181206), Earth System Grid Federation [dataset], https://doi.org/10.22033/ESGF/CMIP6.1391, 2018.

Séférian, R., Nabat, P., Michou, M., Saint-Martin, D., Voldoire, A., Colin, J., Decharme, B., Delire, C., Berthet, S., Chevallier, M., Sénési, S., Franchisteguy, L., Vial, J., Mallet, M., Joetzjer, E., Geoffroy, O., Guérémy, J.-F., Moine, M.-P., Msadek, R., Ribes, A., Rocher, M., Roehrig, R., Salas-y-Mélia, D., Sanchez, E., Terray, L., Valcke, S., Waldman, R., Aumont, O., Bopp, L., Deshayes, J., Éthé, C., and Madec, G.: Evaluation of CNRM Earth System Model, CNRM-ESM2-1: Role of Earth System Processes in Present-Day and Future Climate, J. Adv. Model. Earth Syst., 11, 4182-4227, https://doi.org/10.1029/2019MS001791, 2019.

Seland, Ø., Bentsen, M., Olivié, D., Toniazzo, T., Gjermundsen, A., Graff, L. S., Debernard, J. B., Gupta, A. K., He, Y. C., Kirkevåg, A., Schwinger, J., Tjiputra, J., Aas, K. S., Bethke, I., Fan, Y., Griesfeller, J., Grini, A., Guo, C., Ilicak, M., Karset, I. H. H., Landgren, O., Liakka, J., Moseid, K. O., Nummelin, A., Spensberger, C., Tang, H., Zhang, Z., Heinze, C., Iversen, T., and Schulz, M.: Overview of the Norwegian Earth System Model (NorESM2) and key climate response of CMIP6 DECK, historical, and scenario simulations, Geosci. Model Dev., 13, 6165-6200, https://doi.org/10.5194/gmd-13-6165-2020, 2020.

Seland, Ø., Bentsen, M., Oliviè, D. J. L., Toniazzo, T., Gjermundsen, A., Graff, L. S., Debernard, J. B., Gupta, A. K., He, Y., Kirkevåg, A., Schwinger, J., Tjiputra, J., Aas, K. S., Bethke, I., Fan, Y., Griesfeller, J., Grini, A., Guo, C., Ilicak, M., Karset, I. H. H., Landgren, O. A., Liakka, J., Moseid, K. O., Nummelin, A., Spensberger, C., Tang, H., Zhang, Z., Heinze, C., Iversen, T., and Schulz, M.: NCC NorESM2-LM model output prepared for CMIP6 CMIP (v20190815), Earth System Grid Federation [dataset], https://doi.org/10.22033/ESGF/CMIP6.502, 2019.

Sellar, A. A., Jones, C. G., Mulcahy, J. P., Tang, Y., Yool, A., Wiltshire, A., O'Connor, F. M., Stringer, M., Hill, R., Palmieri, J., Woodward, S., de Mora, L., Kuhlbrodt, T., Rumbold, S. T., Kelley, D. I., Ellis, R., Johnson, C. E., Walton, J., Abraham, N. L., Andrews, M. B., Andrews, T., Archibald, A. T., Berthou, S., Burke, E., Blockley, E., Carslaw, K., Dalvi, M., Edwards, J., Folberth, G. A., Gedney, N., Griffiths, P. T., Harper, A. B., Hendry, M. A., Hewitt, A. J., Johnson, B., Jones, A., Jones, C. D., Keeble, J., Liddicoat, S., Morgenstern, O., Parker, R. J., Predoi, V., Robertson, E., Siahaan, A., Smith, R. S., Swaminathan, R., Woodhouse, M. T., Zeng, G., and Zerroukat, M.: UKESM1: Description and Evaluation of the U.K. Earth System Model, J. Adv. Model. Earth Syst., 11, 4513-4558, https://doi.org/10.1029/2019MS001739, 2019.

Sen, P. K.: Estimates of the Regression Coefficient Based on Kendall's Tau, J. Am. Stat. Assoc., 63, 1379-1389, https://doi.org/10.1080/01621459.1968.10480934, 1968.

Tang, Y., Rumbold, S., Ellis, R., Kelley, D., Mulcahy, J., Sellar, A., Walton, J., and Jones, C.: MOHC UKESM1.0-LL model output prepared for CMIP6 CMIP (v20191011), Earth System Grid Federation [dataset], https://doi.org/10.22033/ESGF/CMIP6.1569, 2019.

Tegen, I., Neubauer, D., Ferrachat, S., Siegenthaler-Le Drian, C., Bey, I., Schutgens, N., Stier, P., Watson-Parris, D., Stanelle, T., Schmidt, H., Rast, S., Kokkola, H., Schultz, M., Schroeder, S., Daskalakis, N., Barthel, S., Heinold, B., and Lohmann, U.: The global aerosol–climate model ECHAM6.3–HAM2.3 – Part 1: Aerosol evaluation, Geosci. Model Dev., 12, 1643-1677, https://doi.org/10.5194/gmd-12-1643-2019, 2019.

Theil, H.: A Rank-Invariant Method of Linear and Polynomial Regression Analysis, Proc. R. Neth. Acad. Sci., 386–392, 1950.

Tilmes, S., Hodzic, A., Emmons, L. K., Mills, M. J., Gettelman, A., Kinnison, D. E., Park, M., Lamarque, J.-F., Vitt, F., Shrivastava, M., Campuzano-Jost, P., Jimenez, J. L., and Liu, X.: Climate Forcing and Trends of Organic Aerosols in the Community Earth System Model (CESM2), J. Adv. Model. Earth Syst., 11, 4323-4351, https://doi.org/10.1029/2019MS001827, 2019.

van Noije, T., Bergman, T., Le Sager, P., O'Donnell, D., Makkonen, R., Gonçalves-Ageitos, M., Döscher, R., Fladrich, U., von Hardenberg, J., Keskinen, J. P., Korhonen, H., Laakso, A., Myriokefalitakis, S., Ollinaho, P., Pérez García-Pando, C., Reerink, T., Schrödner, R., Wyser, K., and Yang, S.: EC-Earth3-AerChem: a global climate model with interactive aerosols and atmospheric chemistry participating in CMIP6, Geosci. Model Dev., 14, 5637-5668, https://doi.org/10.5194/gmd-14-5637-2021, 2021.

Wu, T., Zhang, F., Zhang, J., Jie, W., Zhang, Y., Wu, F., Li, L., Yan, J., Liu, X., Lu, X., Tan, H., Zhang, L., Wang, J., and Hu, A.: Beijing Climate Center Earth System Model version 1 (BCC-ESM1): model description and evaluation of aerosol simulations, Geosci. Model Dev., 13, 977-1005, https://doi.org/10.5194/gmd-13-977-2020, 2020.

Wu, T., Lu, Y., Fang, Y., Xin, X., Li, L., Li, W., Jie, W., Zhang, J., Liu, Y., Zhang, L., Zhang, F., Zhang, Y., Wu, F., Li, J., Chu, M., Wang, Z., Shi, X., Liu, X., Wei, M., Huang, A., Zhang, Y., and Liu, X.: The Beijing Climate Center Climate System Model (BCC-CSM): the main progress from CMIP5 to CMIP6, Geosci. Model Dev., 12, 1573-1600, https://doi.org/10.5194/gmd-12-1573-2019, 2019.

Yukimoto, S., Koshiro, T., Kawai, H., Oshima, N., Yoshida, K., Urakawa, S., Tsujino, H., Deushi, M., Tanaka, T., Hosaka, M., Yoshimura, H., Shindo, E., Mizuta, R., Ishii, M., Obata, A., and Adachi, Y.: MRI MRI-ESM2.0 model output prepared for CMIP6 CMIP historical (v20200218), Earth System Grid Federation [dataset], https://doi.org/10.22033/ESGF/CMIP6.6842, 2019a.

Yukimoto, S., Kawai, H., Koshiro, T., Oshima, N., Yoshida, K., Urakawa, S., Tsujino, H., Deushi, M., Tanaka, T., Hosaka, M., Yabu, S., Yoshimura, H., Shindo, E., Mizuta, R., Obata, A., Adachi, Y., and Ishii, M.: The Meteorological Research Institute Earth System Model Version 2.0, MRI-ESM2.0: Description and Basic Evaluation of the Physical Component, J. Meteorol. Soc. Jpn., 97, 931-965, https://doi.org/10.2151/jmsj.2019-051, 2019b.

Zhang, J., Wu, T., Shi, X., Zhang, F., Li, J., Chu, M., Liu, Q., Yan, J., Ma, Q., and Wei, M.: BCC BCC-ESM1 model output prepared for CMIP6 CMIP (v20191127), Earth System Grid Federation [dataset], https://doi.org/10.22033/ESGF/CMIP6.1734, 2018.